JOURNAL OF SPACECRAFT AND ROCKETS
Vol. 32, No. 6, November–December 1995

Near-Optimal Propulsion-System Operation for an Air-Breathing Launch Vehicle

M. D. Ardema*
Santa Clara University, Santa Clara, California 95053
J. V. Bowles†
NASA Ames Research Center, Moffett Field, California 94035
and
T. Whittaker‡
Sterling Software, Moffett Field, California 94035

A methodology for determining the near-optimal operation of the propulsion system of hybrid air-breathing launch vehicles is derived. The method is based on selecting propulsion-system modes and parameters that maximize a certain performance function. This function is derived from consideration of the energy-state model of the aircraft equations of motion. The vehicle model reflects the many interactions and complexities of the multimode air-breathing and rocket engine systems proposed for launch-vehicle use. The method is used to investigate the optimal throttle switching of air-breathing and rocket engine modes, and to investigate the desirability of using liquid-oxygen augmentation in air-breathing engine cycles, the oxygen either carried from takeoff or collected in flight. It is found that the air-breathing engine is always at full throttle, and that the rocket is on full at takeoff and at very high Mach numbers, but off otherwise. Augmentation of the air-breathing engine with stored liquid oxygen is beneficial, but only marginally so.

Nomenclature

A = air collection capture area, ft^2
C = specific fuel consumption, slugs/s per pound of thrust
D = drag, lb
E = specific energy, ft
e = equivalence ratio, the ratio of actual fuel flow rate to stoichiometric fuel flow rate
F = integrand of cost functional, ft/slug
f_v = ratio of component of thrust along velocity vector to total thrust
g = local acceleration due to gravity, ft/s^2
g_s = sea-level acceleration due to gravity, ft/s^2
h = altitude, ft
J = cost functional, ft^2/slug
J' = inverse cost functional, lb
K = fuel mass/volume weighting parameter, lb/ft^3
K^* = optimal value of K
L = lift, lb
m = mass, slug
m_f = total fuel mass, slug
P = specific excess power, ft/s
P_a = atmospheric static pressure, lb/ft^2
Q_1 = oxygen storage functional, ft^2/slug^2
Q_2 = air collection functional, ft^2/slug^2
R = radius of Earth, 20.92×10^6 ft
T = thrust, lb
T_M = maximum thrust available, lb
t = time, s
V = speed, ft/s
V_f = total fuel volume, ft^3
W_{empty} = empty weight, lb
W_{glo} = gross liftoff weight, lb
α = angle of attack, deg
β = engine mass flow rate, slug/s
γ = flight-path angle, deg
δ = thrust offset angle, deg
ϵ = perturbation parameter
η = flow-rate ratio
η_{air} = ratio of oxygen mass to air mass
π = throttle setting
ρ = fuel density, lb/ft^3
ϕ = optimization function, a weighted sum of fuel mass and volume, lb
ψ = throttle switching parameter
Ω_i = components of Coriolis acceleration, s^{-1}

Subscripts

a = airbreather
f = final
H = hydrogen
i = propulsion type i
O = oxygen
r = rocket
s = side force component
v = component along velocity vector
γ = component perpendicular to velocity vector and in vehicle plane of symmetry

Received Aug. 31, 1994; revision received March 15, 1995; accepted for publication March 15, 1995.

*Professor and Chairman, Department of Mechanical Engineering. Associate Fellow AIAA.
†Aerospace Engineer, Mail Stop 237-11. Member AIAA.
‡Programmer/Analyst, Mail Stop 237-11.

Introduction

STUDIES are underway to select the next generation of space launch vehicles. The main incentive is to dramatically reduce the cost of access to space. The key to achieving this goal is thought to be use of vehicle systems that are completely reusable and operationally more like current aircraft than current launch vehicles.

One launch-vehicle candidate is a single-stage-to-orbit (SSTO) airplane that accelerates within the atmosphere with air-breathing engines for a substantial portion of its flight. This concept has been developed under the National Aerospace Plane program.[1] Such an airplane (Fig. 1) is considerably different than any aircraft ever built and flown, and its development presents many challenges, most notably the design and operation of the propulsion system.

This paper presents a method of determining the near-optimal operation of the propulsion system of a SSTO hybrid air-breathing

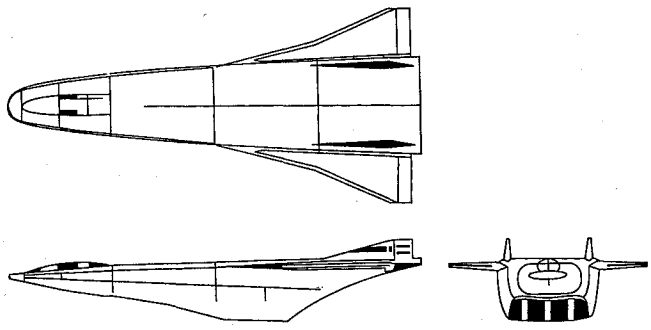

Fig. 1 Single-stage-to-orbit ABLV.

launch vehicle (ABLV). The method is suitable for use in a vehicle synthesis or preliminary design computer code, where ease of use and minimal calculation time are required. It would also be suitable as an on-board automatic propulsion-system controller.

Several authors have developed simplified trajectory analyses for ABLVs, and most of these include propulsion-system optimization schemes.[2–6] All of these analyses are based on reduced-order modeling, and most employ the energy-state approximation. The approach in this paper is an extension and refinement of the method developed in Refs. 5 and 6.

Analysis of ABLV engine operation must take account of the following features (most are unique to hypersonic vehicles):

1) Because of the wide speed range of the vehicle, several different engine types are required; typically these are a low-speed turbomachinery system, a ramjet, a scramjet, and a rocket. The performance of one engine type is often dependent on the performance of another type, which may be in operation simultaneously.

2) An engine type may have several modes of operation. For example, the flow of air into the scramjet may be augmented with liquid oxygen (LOX); this LOX may be carried in tanks at takeoff or may be collected from the atmosphere at lower speeds. As another example, the rocket engine may be of dual-fuel type, that is, able to burn two propellant fuels simultaneously in a controllable ratio.

3) The scramjet engine requires a minimum fuel flow rate for cooling of the engine–airframe structure. The cooling flow requirement depends on speed, altitude, amount of LOX augmentation, and several other variables, and can be as much as three times the flow required for stoichiometric combustion at higher Mach numbers.

4) Vehicle angle of attack has a strong affect on air-breathing engine thrust; because the forebody acts as an inlet ramp, the mass capture of the engine is nearly directly proportional to α.

5) Many of the engine types have a net thrust vector that makes a significant angle with the vehicle longitudinal centerline, up to as much as 50 deg. This decreases the thrust along the velocity vector, affects the required aerodynamic lift, and influences the performance of other engine types through α effects.

6) Because of the low density of liquid hydrogen (LH_2) fuel, hypersonic vehicles are sensitive to fuel volume as well as fuel mass. Consequently, both must be allowed for in any optimization criteria.

The analyses of Refs. 2–4 each include some, but not all, of these features. Our approach incorporates all six. This is accomplished by a suitable choice of cost functional and by modeling the vehicle with the Hypersonic Air Vehicle Optimization Code (HAVOC), briefly described in Refs. 5 and 6. This code has been developed specifically to model the interdisciplinary interactions in hypersonic aircraft and to provide accurate preliminary estimates of vehicle performance. It has been validated by extensive comparison with detailed hypersonic vehicle designs.

Angle-of-attack variations affect mainly mass capture of the air-breathing engine (because the vehicle forebody acts as the compression surface), with secondary effect on inlet kinetic energy efficiency and hence cycle specific impulse. The propulsion model in HAVOC computes two-dimensional keel-line mass capture as a function of freestream Mach number, forebody geometry, and inlet cowl position. Since the angle of attack typically varies between 0 and 5 deg, variations in cycle specific impulse with angle of attack have been neglected.

Selection of the size of the air-breathing engine is a compromise between mass capture requirements for thrust (i.e., acceleration requirements) and propulsion-system weight. The latter is important because hypersonic-engine unit weights are significantly higher than those for typical aircraft structures, due to high design pressure and temperature. In HAVOC, engine width and shock-on-lip Mach number determine engine size, and were based on comparable transatmospheric engine designs. The thrust-to-weight ratio of the rocket was selected to meet takeoff requirements.

In this paper, HAVOC is used to determine the near-optimal operation of the various multimode engine types. In particular, we determine the trajectory points where the rocket and air-breathing engines should be turned on and off, and where LOX augmentation should be used in the scramjet.

Derivation of Propulsion-System Optimization Function

The derivation begins with the singularly perturbed equations of motion of a point-mass airplane with the following assumptions: 1) the aircraft flies in a great circle about a spherical, rotating Earth (terms in the square of the Earth's rotational speed are neglected), 2) the time rate of change of the flight path angle is neglected, 3) the effect of sideslip on vehicle drag is ignored (sideslip is necessary to maintain great-circle flight over a rotating Earth), and 4) there are no ambient winds. Under these assumptions, the equations are

$$\begin{aligned} \epsilon \dot{h} &= V \sin\gamma \\ \dot{E} &= (V/mg_s)(T_V - D) = P \\ \dot{m} &= -\beta \\ 0 &= \frac{V\cos\gamma}{R+h} - \frac{g\cos\gamma}{V} + \frac{T_\gamma + L}{mV} + 2Q_\gamma \\ 0 &= T_s - 2m(Q_r V\cos\gamma - Q_T V\sin\gamma) \end{aligned} \tag{1}$$

Energy, altitude, and velocity are related by the equation

$$E = \frac{hR}{R+h} + \frac{1}{2g_s}V^2 \tag{2}$$

Equations (1) with $\epsilon = 1$ are the trajectory equations in the HAVOC code.

Consistent with this point-mass vehicle model, the trajectory is flown untrimmed. Auxiliary calculations have shown that although the ram drag and gross thrust vectors are large, their moments tend to cancel out. This results in relatively moderate pitching moments, and the vehicle can be trimmed along the entire trajectory.

In Eqs. (1), the singular perturbation parameter ϵ has been inserted in such a way as to give the energy-state approximation when $\epsilon = 0$:

$$\begin{aligned} \dot{E} &= P \\ \dot{m} &= -\beta \end{aligned} \tag{3}$$

To be useful, these equations must be dependent only on altitude and speed. In general, however, P also depends on α, which couples the energy-state equation to the other equations in Eqs. (1). In subsonic aircraft, this dependence is generally eliminated by assuming that the thrust vector is aligned with the velocity vector and by evaluating the drag with lift equalized to weight. For hypersonic aircraft, however, the dependence of P on α is quite complicated and significant. First, the thrust vector is considerably offset from the velocity vector, and it is only the component along the velocity vector that affects P. Second, the thrust magnitude for the air-breathing engine also depends on α, because α affects the mass capture area and thus the airflow into the engine. Finally, if both a rocket engine and an air-breathing engine are operating simultaneously, the rocket throttle setting affects airbreather thrust through α effects. All of these effects are allowed for in the present paper, and, consistent with the energy-state approximation, the value of α used to evaluate P is determined by enforcing equilibrium in the airplane plane of symmetry perpendicular to the velocity vector.

For a SSTO mission with a hypersonic aircraft, what is desired is a trajectory that gives the minimum gross takeoff weight, or the minimum empty weight, to put a given payload mass and volume in orbit. Because LH_2-fueled aircraft have relatively low gross densities and correspondingly high ratios of surface area to gross weight, these aircraft are sensitive to perturbations in volume as well as in mass; it is therefore necessary to minimize a weighted sum of fuel mass and volume. Thus, the quantity to be minimized is

$$\phi = m_f g_s + K V_f \tag{4}$$

Another feature of ABLVs that needs to be taken into account is that they have typically several (more or less) independent propulsion types. If there are n types, the total thrust (along the velocity vector) and fuel flow rates are

$$\begin{aligned} T_v &= f_v \sum_{i=1}^{n} \pi_i T_{Mi} \cos(\alpha + \delta_i) \\ \beta &= \sum_{i=1}^{n} \beta_i = \sum_{i=1}^{n} C_i \pi_i T_{Mi} \end{aligned} \tag{5}$$

The quantity to be minimized for a given energy gain is

$$J' = \int_{\phi_0}^{\phi_f} \mathrm{d}\phi = \int_{t_0}^{t_f} \dot{\phi}\, \mathrm{d}t = \int_{E_0}^{E_f} \frac{\dot{\phi}}{P}\, \mathrm{d}E \tag{6}$$

where Eq. (3) was used. It is assumed that $\dot{\phi} > 0$, $P > 0$, and E is monotonically increasing. If the propellent density is $\rho = m_f g_s / V_f$, then from Eqs. (3) and (4),

$$\dot{\phi} = \dot{m}_f g_s + K \frac{\dot{m}_f g_s}{\rho} = \sum_{i=1}^{n} \beta_i g_s \left(1 + \frac{K}{\rho_i}\right) \tag{7}$$

For convenience, we choose to invert the integrand in Eq. (6) and maximize; from Eqs. (1) and (5–7), the quantity to be maximized is

$$J = \int_{E_0}^{E_f} F\, \mathrm{d}E \tag{8}$$

where

$$F = \frac{V\left[f_v \sum_{i=1}^{n} \pi_i T_{Mi} \cos(\alpha + \delta_i) - D\right]}{m g_s \sum_{i=1}^{n} C_i \pi_i T_{Mi} (1 + K/\rho_i)} \tag{9}$$

If propulsion type i has two propellants (one of which may be LOX) with densities ρ_{1i} and ρ_{2i}, and the ratio of flow rates is $\eta_i = \dot{m}_{1i}/\dot{m}_{2i}$, then the density to be used in Eq. (9) is

$$\rho_i = \frac{\rho_{1i}\rho_{2i}(1 + \eta_i)}{\rho_{1i} + \eta_i \rho_{2i}} \tag{10}$$

The vehicle angle of attack used in evaluating Eq. (9) is determined by enforcing vertical equilibrium [see Eq. (1)]:

$$0 = \frac{V}{R + h} - \frac{g}{V} + \frac{T_\gamma + L}{mV} + 2Q_\gamma \tag{11}$$

Equations (8) and (9) may be used in many ways to study near-optimal ABLV design and operation. For example, if h (and a corresponding V) is chosen at each energy level to maximize F, then a near-optimal flight path, called the energy-climb path, is developed (see Refs. 5 and 6, for example). As another example, if two independent propulsion systems are available at one point in the flight envelope, evaluation of F will indicate which one, or both, should be operated. As a more complicated example, if an air-breathing engine uses LOX augmentation at one point in the climb path, the performance at other parts of the trajectory is affected because of the additional weight and volume of the LOX and its tankage; this type of analysis requires the evaluation of the functional J.

In this paper, the flight path will be fixed, as shown in Fig. 2, and attention will be focused on the operation of the propulsion system. Two representative problems will be studied to illustrate the approach. First, the near-optimal throttle switching between air-breathing and rocket engines will be determined, and second, near-optimal use of LOX augmentation in the scramjet engine will be addressed. The flight path is for a launch due east at latitude 35° and then acceleration to Mach 25.265 following dynamic pressure and heating constraints.

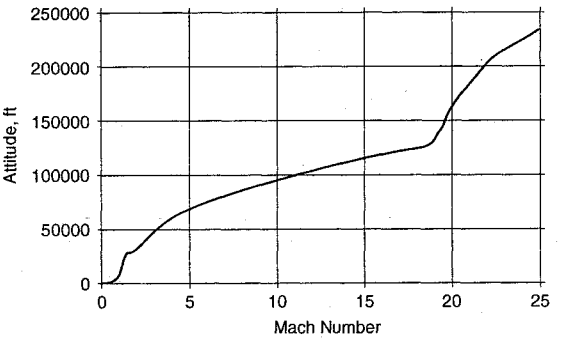

Fig. 2 ABLV trajectory.

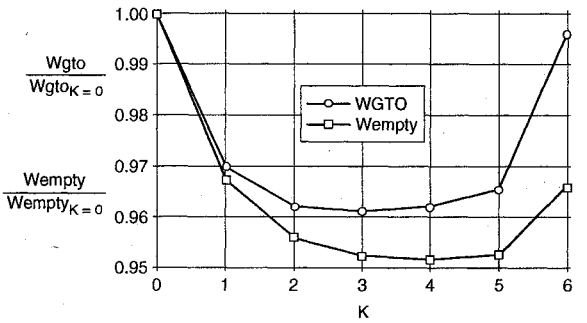

Fig. 3 Effect of weighting parameter K.

Before proceeding with these analyses, the optimal value of K will be determined. This is done numerically by computing closed vehicles for a range of values of K, that is, iteratively exercising the HAVOC code to obtain the gross takeoff weight and volume required to put a specified payload weight and volume in the specified orbit. Because the throttle switchings are changing during these iterations, the propellent bulk density is changing as well. The result for a typical ABLV is shown in Fig. 3. It is seen that, with fuel density in lb/ft^3, a value of $K = 3$, denoted hereafter by K^*, gives very nearly a minimum of both takeoff weight and empty weight, and this value will be used throughout the rest of the paper. The figure shows that use of the optimally weighted cost functional saves 4% in gross weight and 5% in empty weight, relative to minimizing fuel weight only.

Optimal Airbreather–Rocket Throttle Switching

Now assume that there are two independent propulsion types, an air-breathing engine and a rocket engine. It is desired to develop an algorithm for optimal throttle selection for the two types. This problem has been addressed in Refs. 1–3, 5, and 6. In this section, the approach of Refs. 5 and 6 is reviewed and extended.

The function F is now

$$F = \frac{V[f_v \pi_a T_{Ma} \cos(\alpha + \delta_a) + f_v \pi_r T_{Mr} \cos(\alpha + \delta_r) - D]}{m g_s [C_a \pi_a T_{Ma}(1 + K/\rho_a) + C_r \pi_r T_{Mr}(1 + K/\rho_r)]} \tag{12}$$

The controls are now the throttle settings, $\pi_a \in [0, 1]$ and $\pi_r \in [0, 1]$. If ρ_H and ρ_O are the densities of LH_2 and LOX, respectively, then $\rho_a = \rho_H$ and, from Eq. (10),

$$\rho_r = \frac{\rho_O \rho_H (1 + \eta_r)}{\rho_O + \eta_r \rho_H} \tag{13}$$

where η_r is the oxidizer-to-fuel flow ratio of the rocket.

The constraints on the controls will now be discussed. Figure 4 shows the constraints on the throttle settings. Figure 4a shows the equivalence ratio e as a function of freestream Mach number for the air-breathing engine. The resultant thrust from the air-breathing

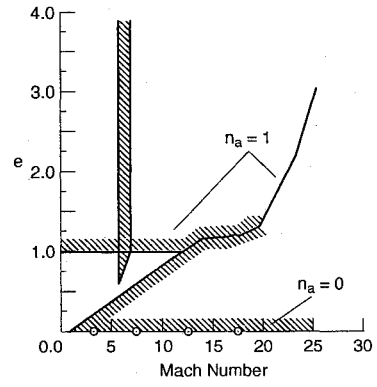

a) Air breather

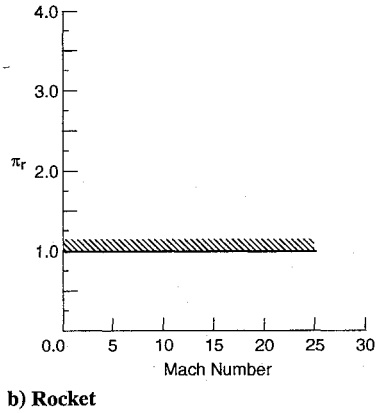

b) Rocket

Fig. 4 Constraints on throttle controls.

propulsion system is then the product of four variables: the equivalence ratio, the stoichiometric fuel-to-air ratio, the air mass flow rate captured by the engine, and the cycle specific impulse. The stoichiometric fuel-to-air ratio is a function of the fuel type. The air capture rate is computed as a function of Mach number, freestream dynamic pressure, angle of attack, and forebody–cowl geometry. The specific impulse is strongly dependent on freestream Mach number and engine equivalence ratio, and only moderately dependent on dynamic pressure and angle of attack. In this analysis, the specific impulse is modeled only as a function of Mach number at full throttle setting ($\pi_a = 1$). This approximation will give acceptable engineering modeling of the airbreather performance.

For Mach numbers less than 6.0, the engine operates in the ramjet mode. In this mode, the engine could be operated over a wide range of equivalence ratios, with a lower bound imposed by required engine–airframe-cooling fuel flow rate, which in general is a function of Mach number and altitude (i.e., dynamic pressure). If there are no other considerations than combustion efficiency, it is not optimum to have $e > 1$; thus, the upper limit $e \leq 1$ is imposed. At Mach 6, the start of the supersonic combustion ramjet mode, there is a pronounced reduction in the allowable engine equivalence ratio due to engine operating limits on the thermal-choke–burner-exit Mach number for the limited-variable-geometry scramjet engines. The net result is a sharp dip in the upper bound for the air-breathing engine to limit heat release in the combustor, as shown in Fig. 4a. As the Mach number is increased in the scramjet mode, this constraint vanishes and the engine is again allowed to burn stoichiometrically. At approximately Mach 12, the airframe–engine cooling requirement determines the required engine fuel flow rate, and hence the equivalence ratio must be greater than the stoichiometric value $e = 1$. In general, the engine equivalence ratio required for cooling will be a function of Mach number and dynamic pressure, with a mild dependence on angle of attack. In this analysis, the angle-of-attack dependence was ignored and the cooling equivalence ratio was computed at the resultant dynamic pressure constrained by the limit on the equilibrium radiation temperature of the forebody compression-ramp surface, which turns out to yield the optimal trajectory in the scramjet operating mode.

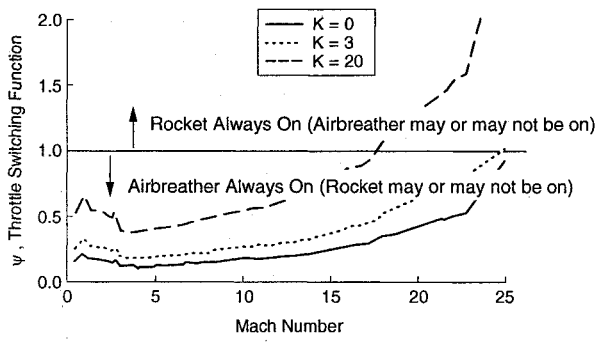

Fig. 5 Throttle-switching test function.

One option always is to turn the air-breathing engine completely off. This is represented by the lower bound of $\pi_a = 0$. For this option, the scramjet duct is closed off using the variable cowl geometry; no engine-cooling fuel flow is required, since the external cowl surface is radiatively cooled. All of these constraints and requirements define the set of admissible controls, and result in the definitions of $\pi_a = 1$ and $\pi_a = 0$, shown in Fig. 4a. The bounds on the throttle setting of the rocket engine, Fig. 4b, are straightforward.

The maximization of F as given by Eq. (12) will now be given. Let

$$\psi = \frac{C_a(1 + K/\rho_a)\cos(\alpha + \delta_r)}{C_r(1 + K/\rho_r)\cos(\alpha + \delta_a)} \tag{14}$$

Then the optimal throttle selection control law is as follows: If $\psi \geq 1$, then

$$\pi_r = 1$$

$$\pi_a = \begin{cases} 0 & \text{if } 1 - \dfrac{D}{f_v T_{Mr}\cos(\alpha + \delta_r)} > \dfrac{1}{\psi} \\ 1 & \text{otherwise} \end{cases} \tag{15a}$$

If $\psi < 1$, then

$$\pi_a = 1$$

$$\pi_r = \begin{cases} 0 & \text{if } 1 - \dfrac{D}{f_v T_{Ma}\cos(\alpha + \delta_a)} > \psi \\ 1 & \text{otherwise} \end{cases} \tag{15b}$$

This control law may be interpreted as follows. First, the engine type that is most fuel-efficient (in terms of optimally weighted mass and volume flow rates) in generating thrust along the velocity vector is turned on (the test on ψ); call this type 1. Then, type 2 is turned on, additionally, if a second test is satisfied. This second test depends on both the thrust-to-drag ratio of type-1 operation, and the relative efficiencies of the two types. Note that if the thrust of type 1 is less than the drag, type 2 is always turned on. Note also that both types are always either on full or completely off.

Figure 5 shows the test function as a function of Mach number for three values of K. As expected, increasing the value of K is associated with a greater emphasis on minimizing fuel volume—thus, a greater use of the rocket and a decreasing use of the airbreather. The associated throttle histories are shown on Fig. 6. For $K = 3$ and $K = 0$, the airbreather is on continuously to the end of the trajectory. The rocket comes on at a high hypersonic Mach number, higher for $K = 0$ than for $K = 3$. For $K = 20$, the airbreather is turned off before the end of the trajectory, and the rocket comes on much earlier. In all cases, the rocket is used for takeoff acceleration augmentation; in fact, that is what sizes the rocket.

Scramjet-Engine Liquid-Oxygen Augmentation

Hypersonic air-breathing propulsion systems produce thrust by processing freestream air: compressing the air, typically through a series of external and internal ramps, combusting the high-pressure air with fuel to add heat, and expanding the combustion product gases through a nozzle. If more air is processed, say by flying at higher dynamic pressures, then the engine thrust will be higher. At

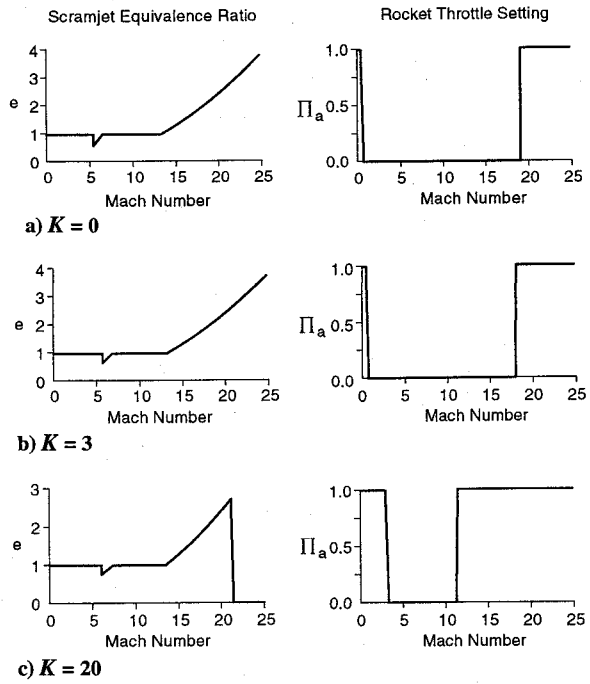

Fig. 6 Optimal throttle schedules.

high Mach numbers, air-breathing hypersonic vehicles encounter increased aerothermal heating, which at first requires the engine fuel flow to be higher than the stoichiometric value to satisfy airframe and engine cooling needs, and eventually forcing the vehicle to fly a lower-dynamic-pressure trajectory dictated by material temperature limits. The resulting higher-altitude, lower-dynamic-pressure flight path results in a decrease in airbreather thrust, which can be compensated for by several means, including use of a rocket engine.

An alternative propulsion enhancement method is the use of oxidizer augmentation and preburning in the hypersonic scramjet engine. In an oxidizer-augmented combustor, fuel is premixed with onboard stored oxidizer in a secondary combustion chamber, and the combustion products are injected into the main airflow path, resulting in improved combustor performance at high Mach numbers, enhanced combustor stream force, and overall higher propulsion system thrust. The higher engine thrust levels are achieved at the expense of higher engine-thrust-specific fuel consumption, due to higher onboard mass flow. Thrust offset angles and engine cooling requirements are changed as well. Burning the fuel with onboard oxidizer, which could be LOX or liquid air, is usually done fuel-rich to assure efficient combustion in the preburner and enhanced mixing of the unburned fuel with the airflow stream in the main combustion chamber. The LOX-augmented engine has higher specific thrust than the liquid-air-augmented one because of its higher combustion temperatures. The oxidizer must be in liquid state to allow combustion in the embedded rocket engine, i.e., the preburner.

The LOX could be stored onboard the vehicle at takeoff, or air collected and liquefied by cryogenic fuel during the ascent. Then, either the scramjet augmentation could use liquid-air preburning, or the oxygen could be separated during the liquefaction process. For the present study, the HAVOC code has been modified to model all these complex interactions involved in LOX-augmented scramjet engine performance.

In this section, we will investigate whether or not this LOX augmentation is beneficial, and, if it is, determine 1) where in the flight path it should be used, 2) how much should be used, and 3) whether it should be carried from the ground or collected en route.

The approach to optimizing the use of LOX augmentation is similar to determining optimal throttle switching: the function F in Eq. (12) is maximized with respect to the amount of augmentation at each point along the flight path. A typical result is shown in Fig. 7. This figure shows the ratio of LOX-to-LH_2 mass flow to the scram jet engine as a function of M. It is seen that LOX augmentation begins at about Mach 18, reaches the maximum allowable level at a slightly higher M, and stays at that level until the end of the flight

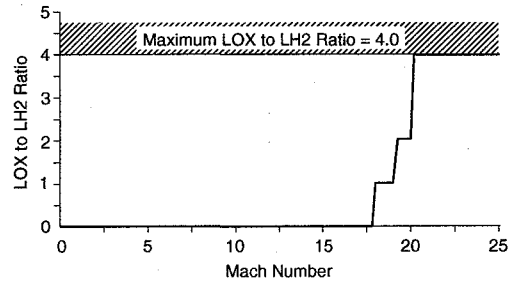

Fig. 7 Optimal LOX augmentation.

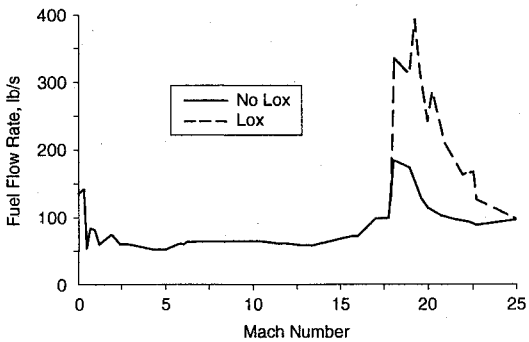

Fig. 8 Fuel flow rates.

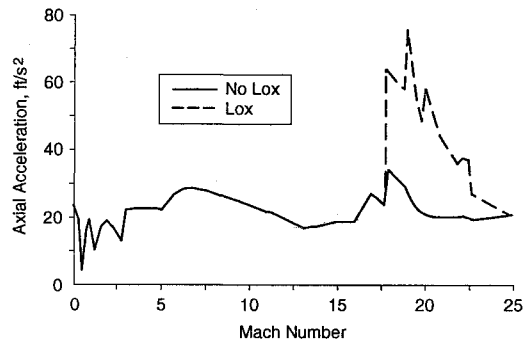

Fig. 9 Axial acceleration.

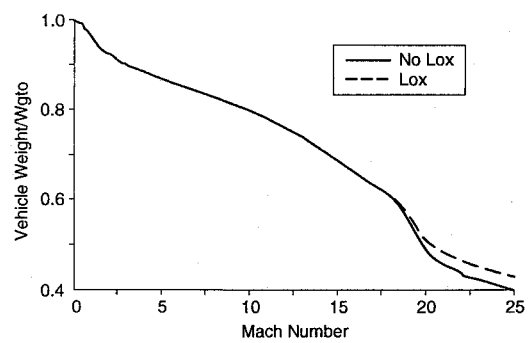

Fig. 10 Vehicle weight with and without LOX augmentation.

path. Figure 8 shows that the fuel rate goes up dramatically when augmentation is used; on the other hand, the longitudinal acceleration also greatly increases (Fig. 9), giving shorter flight times. The net result is that with LOX augmentation a slightly higher final vehicle weight is obtained (as shown on Fig. 10).

It was found that the optimal use of augmentation is highly dependent on the modeled scramjet performance. For example, if the nonaugmented specific fuel consumption is reduced by 10%, or if the augmented fuel consumption is increased by 10%, augmentation is not optimal at any point on the trajectory.

Now consider the issue of whether it is best to store the LOX to be used for augmentation onboard at takeoff, or to collect air during the flight. The latter has the advantage that the takeoff weight will be lower and thus the performance at low speeds will be better,

but the disadvantage that the drag will be higher during air collection. Obviously, air collection will be better when the advantage is greater than the disadvantage. Because two different segments of the trajectory are involved, this issue cannot be decided by pointwise evaluation of the function F; rather, the integrated performance must be evaluated.

Suppose that the trajectory begins at energy level E_0 and that subsequently air is collected in a small interval from E_1 to E_2. The improvement in performance at E_1 due to a change in mass Δm from E_0 to E_1, to first order, is obtained from Eq. (8) as

$$\Delta J_{01} = \left(\frac{dJ}{dm}\Delta m\right)_{01} = \Delta m \int_{E_0}^{E_1} \frac{dF}{dm}\,dE \tag{16}$$

If it is assumed that wing loading is held constant as the airplane changes size and weight, both thrust and drag will tend to change linearly with changes in mass. [The dependence of thrust on mass comes from selecting the angle of attack to balance forces perpendicular to the velocity vector— from Eq. (11)—and from the fact that thrust varies nearly linearly with α.] Thus, from Eq. (9), the only net dependence of F on m is via the explicit factor m, and consequently $dF/dm = -F/m$. Substitution into Eq. (16) gives

$$\Delta J_{01} = -\Delta m \int_{E_0}^{E_1} \frac{F}{m}\,dE \tag{17}$$

This gives the reduction in performance for an increase Δm in vehicle mass.

Next consider the change in performance due to collecting a mass of air Δm_{air} from E_1 to E_2. Again from Eq. (8), to first order,

$$\Delta J_{12} = \left(\frac{dJ}{dm}\Delta m_{\text{air}}\right)_{12} = \Delta m_{\text{air}} \int_{E_1}^{E_2} \frac{dF}{dm}\,dE = \Delta m_{\text{air}} \frac{dF}{dm}\,\Delta E \tag{18}$$

where $\Delta E = E_2 - E_1$ is a small energy increment. Assuming that the only dependence on F of the air collection is through the drag term, we have

$$\frac{dF}{dm} = \frac{dF}{dD}\frac{dD}{dm} \tag{19}$$

From Eq. (9),

$$\frac{dF}{dD} = -\frac{F}{T_v - D} \tag{20}$$

The drag associated with the air collection is

$$D = P_a A + \rho A V^2 \tag{21}$$

where P_a and ρ are the atmospheric static pressure and density, respectively, and A is the collection capture area. Thus

$$\frac{dD}{dm} = P_a \frac{dA}{dm} + \rho \frac{dA}{dm} V^2 \tag{22}$$

The mass captured during time Δt between E_1 and E_2 is $m = \rho A V \Delta t$, so that

$$\frac{dm}{dA} = \rho V \Delta t \tag{23}$$

Combining Eqs. (18–20), (22), and (23) gives

$$\Delta J_{12} = -\Delta m_{\text{air}} \frac{F}{T_v - D} \frac{P_a + \rho V^2}{\rho V} \frac{\Delta E}{\Delta t} \tag{24}$$

From Eqs. (1), $\Delta E/\Delta t = P$, so that Eq. (24) becomes

$$\Delta J_{12} = -\Delta m \frac{F\left(P_a + \rho V^2\right)}{\rho m g_s \eta_{\text{air}}} \tag{25}$$

where all quantities are to be evaluated at E_1, and where η_{air} is the ratio of oxygen mass to air mass ($\eta_{\text{air}} = 0.2315$). Equation (25) gives the reduction in performance due to air collection.

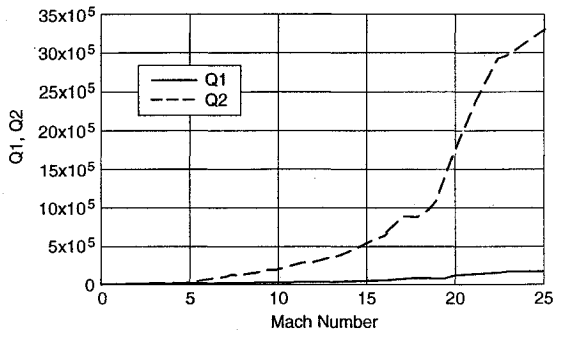

Fig. 11 LOX storage and LOX collection optimization functions.

Now let

$$Q_1 = \int_{E_0}^{E_1} \frac{F}{m}\,dE \tag{26}$$

and

$$Q_2 = \frac{F_1\left(P_{a_1} + \rho_1 V_1^2\right)}{\rho_1 m_1 g_s \eta_{\text{air}}} \tag{27}$$

Then, from Eqs. (17) and (25), air collection will be optimal compared with LOX storage when

$$Q_1 > Q_2 \tag{28}$$

Figure 11 shows the variation of Q_1 and Q_2 along the trajectory. It is seen that the inequality (28) is never satisfied. In fact, the inequality would not be satisfied even if the atmosphere were 100% oxygen, and thus air collection is clearly inferior to LOX storage from takeoff. Also, weight penalties for air liquefaction and disposal of the nitrogen have not been included; if these penalties were included the advantage of LOX storage would increase.

Concluding Remarks

A method based on energy-state approximation has been developed to optimize propulsion-system operation of a single-stage-to-orbit hybrid air-breathing launch vehicle. The cost functional is a weighted sum of propellent mass and volume. To illustrate the method, the optimal throttle switching of rocket and air-breathing engine types was addressed. It was found that, in most cases, the air-breathing engine was at full throttle for the entire ascent trajectory, and the rocket was on for takeoff, then off until a high hypersonic speed, and then on full for the rest of the trajectory.

The use of LOX augmentation in the scramjet engine was also considered. It was found that LOX augmentation is optimal at high hypersonic speeds, but this conclusion is sensitive to scramjet modeling. It was also determined that it is far better to carry the LOX from takeoff than to collect and separate air during flight.

References

[1]Gregory, T., Bowles, J., and Ardema, M., "Two Stage to Orbit Airbreathing and Rocket System for Low Risk, Affordable Access to Space," Society of Automotive Engineers, TP 941168, April 1994.

[2]Corban, J., Calise, A., and Flandro, G., "Rapid Near-Optimal Aerospace Plane Trajectory Generation and Guidance," *Journal of Guidance, Control, and Dynamics*, Vol. 14, No. 6, 1991, p. 1181.

[3]Van Buren, M., and Mease, K., "Aerospace Plane Guidance Using Time-Scale Decomposition and Feedback Linearization," *Journal of Guidance, Control, and Dynamics*, Vol. 15, No. 5, 1992, p. 1166.

[4]Lu, P., "Analytical Solutions to Constrained Hypersonic Flight Trajectories," *Journal of Guidance, Control, and Dynamics*, Vol. 16, No. 5, 1993, p. 956.

[5]Ardema, M., Bowles, J., and Whittaker, T., "Optimal Trajectories for Hypersonic Launch Vehicles," *Dynamics and Control*, Vol. 4, No. 4, 1994, p. 337.

[6]Ardema, M. D., Bowles, J. V., Terjesen, E. J., and Whittaker, T., "Approximate Altitude Transitions for High-Speed Aircraft," *Journal of Guidance, Control, and Dynamics*, Vol. 18, No. 3, 1995, pp. 561–566.

J. A. Martin
Associate Editor